

**Hayabusa 2021 Symposium Schedule (Online Meeting)**  
**(8th ISAS Symposium of the Solar System Materials)**

version. 20211111

16th(Tue)-17th(Wed) of November 2021

Oral : Zoom Meeting (10+5 min for Invited and normal talks, 7+3 min for 10 min short talks)

Poster : Zoom Meeting Breakout Rooms

Non-real time discussion : Slack

**Day-1 (Nov 16th) : Poster Session**

JST	GMT	EST	PST	No.	Title	Author/Presenter	Invited
					Poster Session and chat (2 hours) : R. Fukai, T. Hayashi		
19:15	10:15	05:15	02:15	P-1	The fundamental deformation of cosmic bodies not depending of their sizes and compositions(from asteroids to Universe)	Gennady Gregory Kochemasov	
				P-2	Exogenous copper sulfide in a returned grain from asteroid Itokawa	Katherine D Burgess	
				P-3	A Series of Recent Falls of Carbonaceous Chondrites - Perfect Analogues for Returned Hayabusa 2 and Osiris Rex Asteroidal Materials	Viktor H Hoffmann	
				P-4	Heated Synthetic Murchison Reflectance Spectra	Sahejpal Sidhu	
				P-5	Status of the Curatorial Database System for the Ryugu Samples	Masahiro Nishimura	
				P-6	Methodology of MicrOmega data acquisition/processing in initial description of Ryugu returned samples	Kasumi Yogata	
				P-7	Comparison of ion- and laser-weathered spectra of olivines and pyroxenes	Kateřina Chrbolková	
				P-8	Solid Materials of Mineral and Rock on the Solar System: X-ray Unit and Mixed Status	Yasunori Miura	
				P-9	Model of Material Characteristics of Carbonaceous Meteorites from Texture of Carbon-Bearing Grains	Yasunori Miura	
				P-10	Neural network for classification of asteroid spectra	David Korda	
				P-11	Assessment of organic, inorganic, and microbial contamination in the facilities of the Extraterrestrial Sample Curation Center of JAXA	Yuya Hitomi	

## The fundamental deformation of cosmic bodies not depending of their sizes and compositions (from asteroids to Universe)

Kochemasov G. G. IGEM RAS, Moscow, kochem.36@mail.ru

Abstract: Orbits make structures. Not depending sizes and compositions of celestial bodies they acquire tectonic dichotomy (two hemispheres) connected with warping action of fundamental wave.

Keywords; cosmic bodies. orbits, galaxies, planets, satellites, asteroids, fundamental wave

The main point of the wave planetology is: "Orbits make structures". It means that movement in non-round orbits makes waves creating structures (Fig. 1-10) However, any cosmic body moves in several orbits. They all participate in structuring [1]. Their frequencies are divided and multiplied creating new frequencies and corresponding them structures. They are (frequencies) very small and very big. Very slow but very energetic rotation of large cosmic formations (galaxies and the larger assemblies) make very fine oscillations up to microwaves, roentgen and gamma radiations infilling cosmos. From the other end, oscillations passed through fundamental wave and corresponding it tectonic dichotomy of any body. In figures are examples of bodies of various sizes from the Galaxy to small asteroids (Fig.1-8)

The row is finished with small asteroids Itokawa and Ryugu. Both reveal tectonic dichotomy; especially sharp in Itokawa with its convexo-concave shape. Ryugu has unique longitudinal variation in geomorphology: the western side of it has a smooth surface and a sharp equatorial ridge (bulge) [3]. On the opposite side Fossae Tokoyo and Horai occur. Some peculiarities show crater distribution (more than 20 meters in diameter). There are fewer craters in the western bulge and more around the meridian. This cannot be explained by the randomness of cratering [2].

The other end of this row include giant cosmic formations like galaxies and larger ones finishing at Universe. The Universe also is dichotomist divided at uplifted and subsided halves. The humankind occupies the uplifted halve-in the religious sense "paradise", the subsided halve thus is "hell".

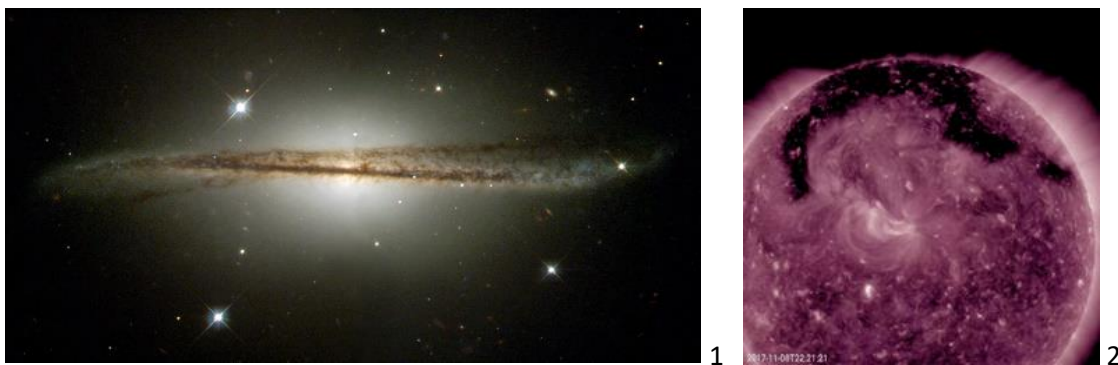


Fig. 1. A spiral Galaxy. ESO 510-613. PIA04213.

Fig.2. PIA22113. Coronal hole all spread out.

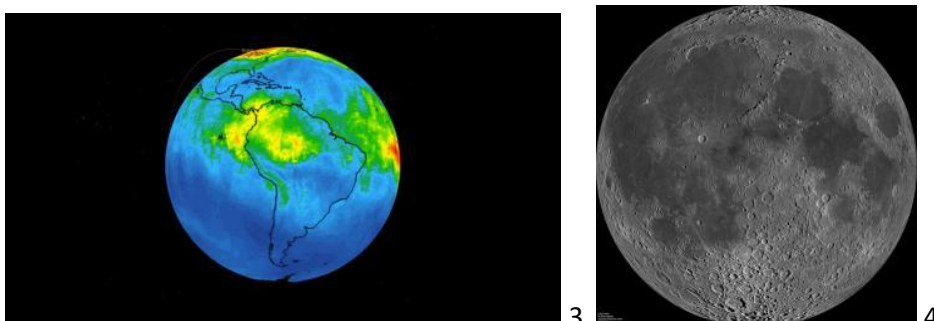


Fig. 3. PIA23356. NASA's AIRS maps carbon monoxide from Brazil fires.

Fig. 4. PIA14011. Moon's nearside

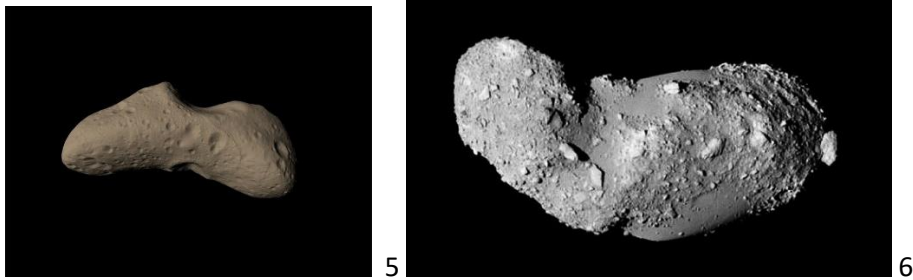


Fig. 5. Asteroid Eros. Convexo-concave shape.

Fig. 6. Asteroid Itokawa. Convexo-concave shape.

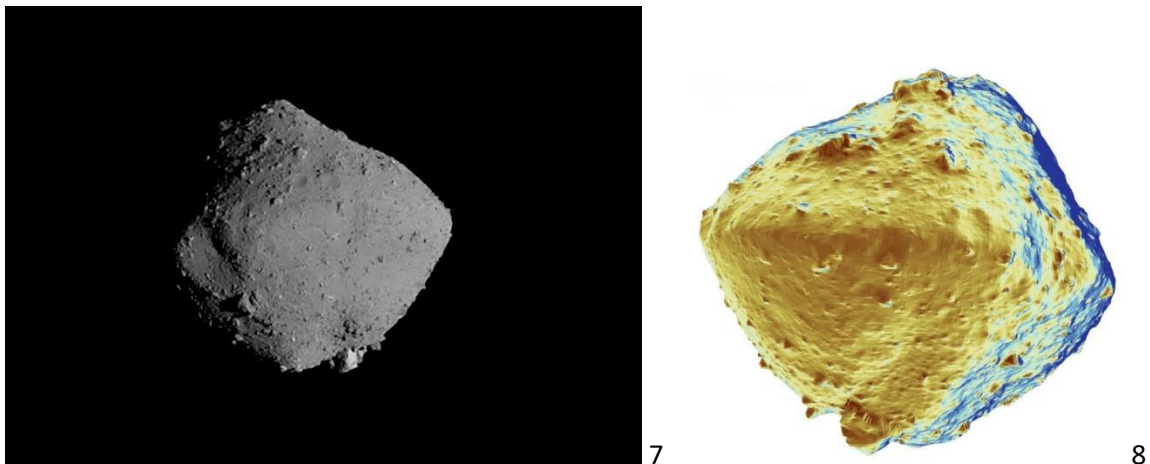


Fig. 7. Asteroid Ryugu. Ab278776d6ce43e581d669ef938497fa.jpg

Fig. 8. Asteroid Ryugu. Dichotomy shows.image\_5c91c15458e6c0.69646182.jpg

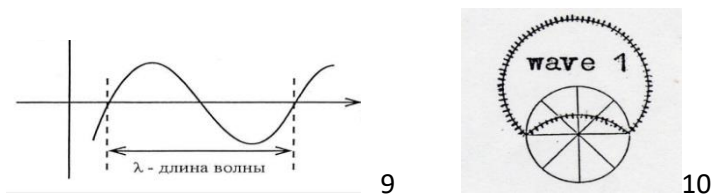


Fig.9, 10. Fundamental wave in line and circle.

#### Referencs:

- [1] Kochemasov G.G. Modulated wave frequencies in the Solar system and Universe // Journal of Physics and Application 12(4): 68-75, 2018. Doi:10.13189/ujpa.2018.120402.
- [2] N.Hirata, T. Morota, Y.Cho et al. The spatial distribution of impact craters on Ryugu// Icarus , v.338, 1, March 2020, 113527, [https:// doi.org/10.1016/j.icarus.2019.113527](https://doi.org/10.1016/j.icarus.2019.113527)
- [3] ] H. Masatoshi, T. Eri, M. Hideaki et al. The western Bulge of 162173Ryugu formed as a result of a rotationally driven deformation process // The Astronomical Journal: journal-IOP Publishing, 2019-March (vol.874, #1-P. L10.-ISSN 0004-637X-doi:10.3847/2041-8213/ab0e8b-Bibcode: 2019ApJ...874L.10N-arXiv:1904.03480.

# Exogenous copper sulfide in a returned grain from asteroid Itokawa

K. D. Burgess and R. M. Stroud

U.S. Naval Research Laboratory, Washington, DC 20375

Asteroid 25143 Itokawa is an S-type asteroid, and the returned samples are dominated by equilibrated, weakly shocked LL5 and LL6 ordinary chondrite material with some weakly equilibrated LL4 material [1,2]. We present evidence of the presence of a cubanite-chalcopyrite-pyrrhotite-troilite assemblage consistent with low-temperature aqueous alteration in a particle from Itokawa [3]. Most of the materials from Itokawa equilibrated at temperatures near 800°C, with slow cooling to ~600°C [2,4], which indicates this sulfide assemblage must have become part of Itokawa after thermal alteration. Cu-bearing sulfides have been reported in only a few meteorite types [5,6], which suggests the conditions necessary to form such phases occur on only a limited number of planetary bodies. Specifically, cubanite has only been reported in CI chondrites and Wild2 material [7]. Thus, we conclude that this grain, and the other Cu-sulfides noted on Itokawa samples [8] likely originated on a primitive, hydrated asteroid source such as CI chondrite-like parent body or D- or P-type asteroids previously linked to unique, aqueously altered meteorites [9,10].

Particle RB-CV-0038 (C0038) was mounted in epoxy such that most of the grain was available for imaging, then coated by 80 nm of evaporated carbon. SEM images and FIB samples were obtained with an FEI Helios G3 equipped with an Oxford 150 mm<sup>2</sup> SDD energy dispersive X-ray spectrometer (EDS). After imaging, protective straps of C were deposited on regions of interest, and multiple sections suitable for STEM analysis were extracted using standard techniques. One section, known from SEM-EDS to contain Cu, was attached to a Mo grid. STEM analysis was performed with the Nion UltraSTEM200-X at NRL. The microscope is equipped with a Gatan Enfium ER spectrometer for electron energy loss spectroscopy (EELS) and a windowless, 0.7 sr Bruker SDD-EDS detector. Selected area diffraction patterns were collected using a JEOL 2200FS. Data were collected at 200 kV.

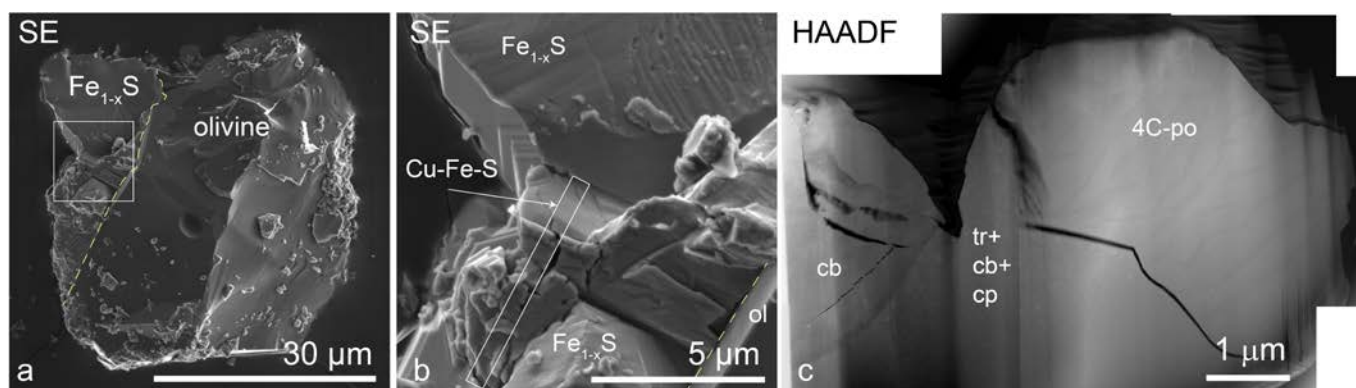


**Figure 1.** (a,b) Secondary electron (SE) images of particle RB-CV-0038 showing location of cubanite with Fe-sulfide and approximate location of FIB section. (c) HAADF montage of FIB section with cubanite (cb), troilite-cubanite-chalcopyrite (tr+cb+cp) mottled region, and pyrrhotite (4C-po) with “flame” texture.

C0038 is a multiphase grain, ~40 μm across. The particle is predominantly composed of olivine and iron sulfide with minor (adhered?) plagioclase or glass (Fig. 1a). A ~2×5 μm cubanite grain was present in contact with the Fe-sulfide (Fig. 1b). STEM data show several different grains are present within the Fe-sulfide in the FIB section (Fig. 1c). The Cu-Fe-sulfide contains several cracks are, one of which is perpendicular to the FIB section (Fig. 2a). The crack has oxidized Fe-rich edges and is decorated by Cu metal nanoparticles. The cubanite itself shows a tripling of the *c* axis, apparent in SAED patterns (Fig. 2b). Adjacent to the cubanite, the sulfide has a mottled texture (Fig. 2a), and a small amount of Cu is present (~2 at%), concentrated in the bright spots. SAED patterns from the region index to troilite with faint chalcopyrite spots (Fig. 2d). Further from the chalcopyrite, there is no Cu, and the Fe-sulfide has a “flame” exsolution texture of two types of pyrrhotite (Fig. 2c). The pyrrhotite can be indexed to 4C-pyrrhotite. The average measured Fe/S composition for the grain ( $x = \sim 0.09$  in  $Fe_{1-x}S$ ) is consistent with a 4C-pyrrhotite or a mixture of 4C and NC-pyrrhotites. In NC-pyrrhotites, NC indicates a variable, non-integral superstructure based on the NiAs-type unit cell where troilite is 2C.

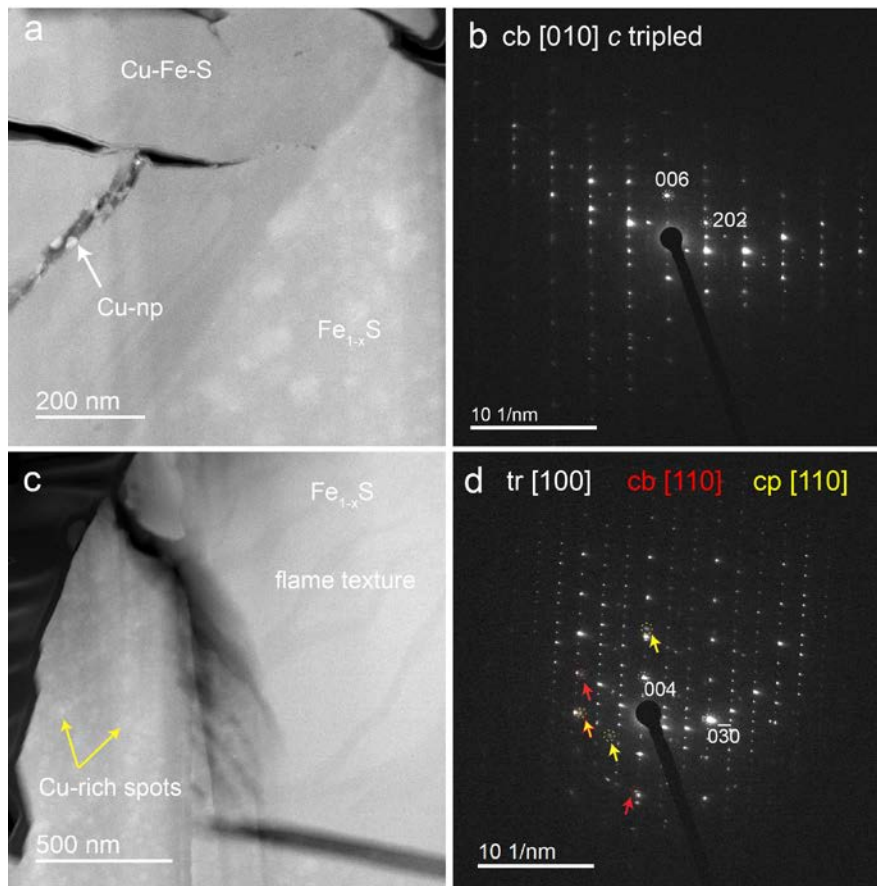


**Figure 2.** (a,c) HAADF images of cubanite, mottled Fe-sulfide, and pyrrhotite with flame texture. (b) SAED pattern for the cubanite, which shows a tripling of the c axis. (d) SAED pattern for the mottled Fe-sulfide, which has ~2 at% Cu and shows reflections for cubanite and chalcopyrite in addition to troilite.

The presence of cubanite, which forms and is stable only at temperatures below ~250°C [11], together in this grain with 4C-pyrrhotite [7], indicates that this grain must have been brought to Itokawa after thermal alteration and equilibration of the LL-type material. This combination of sulfide phases has previously been identified only in CI chondrite material [7]. However, unlike CI chondrites, no Ni was detected in these sulfides. This could indicate variation in the CI parent body, or that the impactor seen here was from a different parent body, such as the aqueously altered D- or P-type asteroids.

### Acknowledgements

The authors thank JAXA and the Hayabusa curation team for access to the samples. Funding was provided by NASA LARS award 80HQTR20T0050 and NNH17AE44I to RMS.

### References

- [1] Mikouchi, T., et al. (2014) *Earth, Planets and Space*, 66, 82. [2] Noguchi, T., et al. (2011) *Science*, 333, 1121. [3] Burgess, K.D., and Stroud, R.M. (2021) *Communications Earth & Environment*, 2, 115. [4] Harries, D., and Langenhorst, F. (2018) *Geochimica et Cosmochimica Acta*, 222, 53. [5] Rubin, A.E. (1997) *Meteoritics & Planetary Science*, 32, 231. [6] Rubin, A.E., and Ma, C. (2017) *Geochemistry*, 77, 325. [7] Berger, E.L., et al. (2011) *Geochimica et Cosmochimica Acta*, 75, 3501. [8] Nakamura, E., et al. (2012) *Proceedings of the National Academy of Sciences of the United States of America*, 109, E624. [9] Brown, P.G., et al. (2000) *Science*, 290, 320. [10] Kebukawa, Y., et al. (2019) *Scientific Reports*, 9, 3169. [11] Dutrizac, J. (1976) *The Canadian Mineralogist*, 14, 172.

## A Series of Recent Falls of Carbonaceous Chondrites - Perfect Analogues for Returned Hayabusa 2 and Osiris Rex Asteroidal Materials

V.H. Hoffmann<sup>1</sup>, K. Wimmer<sup>2</sup>, M. Kaliwoda<sup>1,3</sup>, W. Schmahl<sup>1,3</sup>, P. Schmitt-Kopplin<sup>4</sup>. <sup>1</sup>Faculty of Geosciences, Dep. Earth and Environmental Sciences, Univ. Munich; <sup>2</sup>Nördlingen; <sup>3</sup>Mineralogical State Collection Munich, SNSB; <sup>4</sup>Helmholtz-Center, Munich; Germany.

### Introduction

In recent years, a series of meteorite falls have been reported which produced various types of primitive chondrites. In our contribution we will focus on samples of the following witnessed falls: Flensburg (2019), Kolang and Tarda (both 2020), while Mukundpura (fall 2017) was topic of our earlier studies [1-3]. These meteorites belong to the class of carbonaceous chondrites and play a prominent role in terms of the Hayabusa 2 (successful sample return from asteroid Ryugu in December 2020) and Osiris Rex (sample return from asteroid Bennu planned in 2023) missions [4,5]. Both probed asteroids belong to the C type asteroids and are believed to mainly consist of carbon rich materials with a similar composition as primitive chondrites.

The Flensburg meteorite fell in September 2019 in Northern Germany and was classified as a C1 ungrouped carbonaceous chondrite, the first reported fall of this type. Only one small stone was found so far (24.5 gr). For all further details we refer to [2]. The Tarda meteorite fall was reported from Southern Morocco in August 2020, the meteorite (about 4 kg total mass) was classified as a C2 ungrouped carbonaceous chondrite [1,2,6,7]. Only four witnessed falls of this type are known, whereby Tagish Lake is probably the most famous one (fall 2000, [1]). The Kolang meteorite fireball and fall was reportedly observed in Indonesia in August 2020 (four stones with a total mass of 2550 gr). Kolang was classified as a CM 1/2 chondrite and is the first and only witnessed fall known from this meteorite group [8,9].

In our contribution (poster) we will compile our earlier and provide new results of detailed and systematic investigations on the mineral phase composition and distribution of three new meteorite falls [10,11]. Our focus was mainly on the rare/accessory mineralogical components of these meteorites. Specifically we are interested on the carbon-bearing and the magnetic phases. Several unprepared fragments and one individual of Tarda were used for our studies, and additionally one small unprepared fragment of Kolang. Concerning Flensburg, we had a small fragment and a PTS (provided by A. Bischoff, Univ. Münster). We used optical microscopy, LASER Micro Raman Spectroscopy (Horiba XploRa Raman System, MSM/ SNSB) for our study which is perfectly suited for identifying and mapping minor/accessory phases. Being fully non-destructive, allowing high-resolution mapping on natural, broken surfaces without any preparation in 2D or 3D are some of the major advantages of this technique. The surface morphology and mineralogy of the uncoated samples was investigated using a Phenom ProX scanning electron microscope (SEM) in backscattered electron mode equipped with an energy dispersive X-ray spectrometer (EDS) for analyzing the element composition. Magnetic susceptibility was investigated systematically by an SM30 (Hulka Comp., CR).

The results of our Raman spectroscopy experiments on Kolang have to be seen as preliminary as we had only one small fragment for our project. Generally, performing successful LASER Raman experiments on carbonaceous chondrites, here specifically on Flensburg, Tarda and Kolang, required the design of a highly sophisticated experimental setup to avoid or at least minimize alteration effects already during the measurements on the one hand and to guarantee a reasonable signal/noise relationship on the other. Due to the significant brecciation and very fine grained matrix / phases, experiments on Kolang are quite complex. Generally, several phases which have been detected in these primitive carbonaceous chondrites are extremely sensitive against (even minor) heating effects, and therefore any kind of preparation (cutting/grinding etc.), specifically in terrestrial atmospheric conditions has to be minimized. In order to avoid any such effects we decided to investigate only naturally broken unprepared sample materials (PTS of Flensburg is a necessary exception because of representativity but we also had a fragment). The representativity of the data obtained on the available sample material was also topic of our studies: large sets of high resolution mappings in 2D/3D can help to overcome the problem of tiny samples / fragments. Our experiences from the earlier investigations on Hayabusa 1 materials (asteroid Itokawa) were highly profitable in this context [12-14].

Consequently, our main interests were on optimizing and fine tuning our experimental setup. So the series of recent meteorite falls which produced a new set of primitive carbonaceous chondrites provided us directly with unique fresh analogue materials for Hayabusa 2 and Bennu asteroidal samples in our laboratories. We plan to extend our investigations in near future to additional recent falls such as Aquas Zarcas (2019, Costa Rica, CM2) or most recently Winchcombe (2021, England/UK, CM2) [1,3].

## References

- [1] Meteor. Bull. Database 10/2021: Flensburg , Tarda, Kolang, Aquas Zarcas, Winchcombe, Mukundpura, Tagish Lake.
- [2] Bischoff A. et al., 2021. The old, unique C1 chondrite Flensburg – Insight into the first processes of aqueous alteration, brecciation, and the diversity of water-bearing parent bodies and lithologies. *Geochem. Cosmochem. Acta*, 293, 142-186.
- [3] <https://www.karmaka.de> (10/2021)
- [4] Hayabusa 2 mission to asteroid Ryugu (finished 12/2020), JAXA: <https://www.hayabusa2.jaxa.jp/en/>
- [5] Osiris Rex mission to asteroid Bennu, NASA: <https://www.nasa.gov/osiris-rex>
- [6] Chennaoui H.A., et al., 2021. Tarda (C2-ung): a new and unusual carbonaceous chondrite meteorite fall from Morocco. 52<sup>nd</sup> LPSC 2021, #1928.
- [7] Dey S., et al., 2021. Exploring the planetary genealogy of Tarda – a unique new carbonaceous chondrite. 52<sup>nd</sup> LPSC 2021, # 2517.
- [8] King A.J., et al., 2021. The bulk mineralogy and water contents of the carbonaceous chondrite falls Kolang and Tarda. 52<sup>nd</sup> LPSC 2021, #1909.
- [9] Jenkins L.E., et al., 2021. Identification of clasts in CM chondrite fall Kolang with S and Ca. 84<sup>th</sup> Meteor. Soc. Conf., #6161.
- [10] Hoffmann V., et al., 2021. The Kolang (CM1/2) and Tarda (C2 ungrouped) meteorite falls from 2020: first systematic mineralogical investigations by LASER Raman spectroscopy and SEM/EDX. 52<sup>nd</sup> LPSC 2021, # 2458.
- [11] Hoffmann V., et al., 2021. The Flensburg (C1 ungrouped) 2019 meteorite fall: Raman spectroscopy and compilation of magnetic susceptibility data on C-ungrouped falls/finds. 52<sup>nd</sup> LPSC 2021, # 2443.
- [12] Mikouchi T., Hoffmann V.H. et. al., 2014. Mineralogy and crystallography of some Itokawa particles returned by the Hayabusa mission. LPSC 2021, #2239.
- [13] Mikouchi T., Hoffmann V.H., et al., 2013. Mineralogy and crystallography of Itokawa particles by electron beam and synchrotron radiation X-ray analyses. Hayabusa Conf. 2013.
- [14] Mikouchi T. and Hayabusa Consortium, 2014. Mineralogy and crystallography of some Itokawa particles returned by the Hayabusa asteroidal sample return mission. *Earth, Planets and Space*, 66/82, 9pp.

# Heated Synthetic Murchison Reflectance Spectra

S. Sidhu<sup>1</sup>, P. Mann<sup>2</sup> and E. Cloutis<sup>1</sup>

<sup>1</sup>Centre for Terrestrial and Planetary Exploration (C-TAPE), The University of Winnipeg

<sup>2</sup>Department of Geography, The University of Winnipeg

**Introduction:** Several carbonaceous chondrites (CCs) display evidence of thermal alteration [1]. Remote sensing data from the JAXA Hayabusa2 asteroid sample return mission suggests that asteroid (162173) Ryugu's parent body may have undergone internal or impact-generated heating prior to breakup [2]. Furthermore, models of orbital and thermal evolution of Ryugu suggest that the asteroid was likely exposed to surficial heating during close passes to the Sun. [3]. Recently, geomorphological features observed on Bennu's surface indicate alteration of rocks due to thermal fatigue [4]. Constraining the spectral characteristics of heating will aid in identifying the timing and intensity of heating experienced by Ryugu and its parent body, as well as other extraterrestrial bodies which may have also undergone a period of thermal alteration.

**Methods:** The Centre for Terrestrial and Planetary Exploration (C-TAPE) at the University of Winnipeg conducted a heating experiment on a synthetic Murchison simulant. The synthetic mixture, named WMM, consisted of various major representative phases in CM carbonaceous chondrites as following: 85 wt. % ASB267, a dark serpentinite representative of CM phyllosilicates. 5 wt. % SHU102, shungite, terrestrial organic representative of organic phases. 5 wt. % TRO203, synthetic troilite representative of sulfides, and 5 wt. % MAG200, magnetite. The simulant consisted of <63  $\mu\text{m}$  powders of serpentinite, shungite, and troilite, and ~20 nm sized magnetite that appeared to be maghemite from X-ray diffractometry (likely due to surface oxidation of the nanoparticles). The samples were heated up to 1200°C at 100°C increments. XRD and reflectance spectra were collected prior to heating, and after each temperature increment. A new sample powder was used for each increment, and samples were heated under continuous nitrogen flow. Samples were heated for one week at intervals of 100°C to 1000°C. However, due to the oven's constraints, samples were only heated for 2 hours at 1100°C and half an hour at 1200°C. The reflectance spectrum for 300°C is unavailable due to an accidental sample spill while removing the powder from the oven. The spectra were collected with an Analytical Spectral Devices (Boulder, CO) LabSpec 4 Hi-Res® spectrophotometer between 350 and 2500 nm. Spectra were measured at a viewing geometry of  $i = 30^\circ$  and  $e = 0^\circ$  with incident light being provided by an in-house 150 W quartz-tungsten-halogen collimated light source. Sample spectra were measured relative to a Labsphere Spectralon® 100% diffuse reflectance standard and corrected for minor (less than ~2%) irregularities in its absolute reflectance.

**Results:** Heating the Murchison simulant samples resulted in spectral variation across the temperature increments. The spectra show little change up to ~500°C (Figure 1). Beyond 500°C, the spectra display features associated with Fe<sup>3+</sup> oxyhydroxides, such as low reflectance below ~500nm, a steep red slope in the visible region, and absorption features near 870 nm. Absorption bands associated with serpentine, at 1400 and 2320 nm, are evident up to ~600-700°C. The spectra generally become brighter up to ~800°C, and then darken substantially beyond this temperature. At and above 1100°C, the spectra are generally dark and featureless, with a broad absorption region centered near 1600 nm.

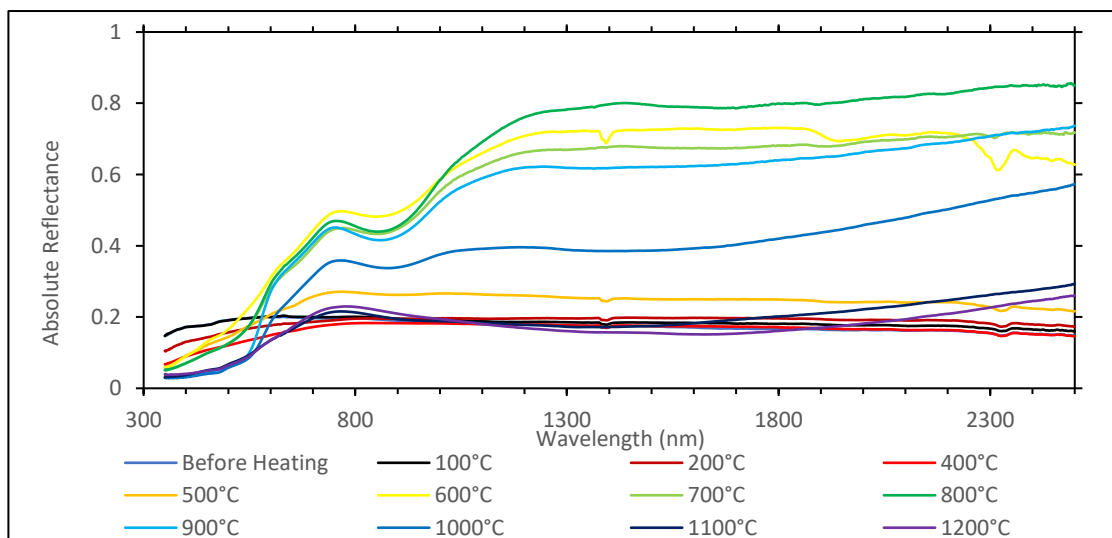


Figure 1. Reflectance Spectra of Simulated Murchison Mixture WMM.

Additionally, we heated end members used to produce the Murchison simulant to better understand the causes of the spectral changes observed. These samples (serpentine, shungite, troilite, and magnetite) were heated under the same conditions as the simulant. Serpentine spectra remained unchanged up to  $\sim 200^{\circ}\text{C}$ , after which the spectra display an increasing red slope below  $\sim 700\text{ nm}$  and an absorption feature near  $860\text{ nm}$ , both of which are ascribed to  $\text{Fe}^{3+}$  oxyhydroxides. Furthermore, the OH absorption bands near  $1400\text{ nm}$  and  $2320\text{ nm}$  associated with serpentine were evident up to  $\sim 700^{\circ}\text{C}$ . Reflectance generally increased up to  $\sim 600^{\circ}\text{C}$ , and decreased at higher temperatures. Shungite was stable up to  $\sim 500^{\circ}\text{C}$ . However, at  $600^{\circ}\text{C}$ , the organic component of the sample was volatilized. Troilite remained stable up to  $\sim 300^{\circ}\text{C}$ , after which  $\text{Fe}^{3+}$  oxyhydroxides were evident in its spectra. Fine-grained magnetite remained stable up to  $\sim 100^{\circ}\text{C}$ , after which it also transformed to  $\text{Fe}^{3+}$  oxyhydroxides.

**Discussion:** Temperature-induced spectral changes are evident in the Murchison simulant used in this study. XRD measurements confirm that the changes seen in the spectra can be related to the changes in the mineralogy of the samples. The spectral changes occur in multiple wavelength regions, suggesting that various spectral metrics could be robust indicators of temperatures experienced by a serpentine-rich carbonaceous chondrite.

Spectral changes observed in this study are associated with short heating periods (hours to days), and are thus, applicable to short-term heating events such as impact heating. The applicability of these results to long-term heating events, such as internal heating within larger asteroids, is unknown. Furthermore, the dry nitrogen environment under which this heating experiment was conducted only represents one scenario of the conditions which may have prevailed on carbonaceous chondrite parent bodies during any heating events. Nevertheless, the results of our experiments suggest that spectroscopic data in the  $350\text{-}2500\text{ nm}$  can provide insights into the intensity and duration of heating events affecting carbonaceous chondrite asteroids. It is also worth noting that naturally-heated carbonaceous chondrites show spectral differences associated with changes in mineralogy [1]. We are in the process of relating the results of these experiments to other carbonaceous chondrite heating experiments [5, 6, 7, 8] and naturally-heated carbonaceous chondrites [9] to better understand the full applicability of our results to observational data.

## References

- [1] Cloutis E. et al. 2012. *Icarus* 220:586-617. [2] Sugita S. et al. 2019. *Science* 6437:252. [3] Michel P. & Delbo M. 2010. *Icarus* 209:520-534. [4] Molaro J.L. et al. 2020. *Nature Communications* 11:2913. [5] Hiroi T. et al. 1993. *Science* 261:1016-1018. [6] Hiroi T. et al. 1993. *Symposium on Antarctic Meteorites* 18:93-96. [7] Hiroi T. et al. 1994. *Proceedings of the NIPR Symposium on Antarctic Meteorites* 7:230-243. [8] Hiroi T. et al. 1996. *Meteoritics and Planetary Science* 31:321-327. [9] Hiroi T. et al. 1997. *Lunar and Planetary Science Conference* 28:577-578.

## Status of the Curatorial Database System for the Ryugu Samples

M. Nishimura<sup>1</sup>, T. Yada<sup>1</sup>, M. Abe<sup>1</sup>, A. Nakato<sup>1</sup>, K. Yogata<sup>1</sup>, A. Miyazaki<sup>1</sup>, K. Kumagai<sup>2</sup>, K. Hatakeda<sup>2</sup>,  
T. Okada<sup>1</sup>, Y. Hitomi<sup>2</sup>, H. Soejima<sup>2</sup>, K. Nagashima<sup>1</sup>, T. Usui<sup>1,3</sup>, and S. Tachibana<sup>1,3</sup>

<sup>1</sup>*Inst. Space Astronaut. Sci. (ISAS), Japan Aerosp. Explor. Agency (JAXA), Kanagawa 252-5210, Japan*  
(nishimura.masahiro2@jaxa.jp), Japan, <sup>2</sup>*Marine Works Japan Ltd., Yokosuka 237-0063, Japan*, <sup>3</sup>*UTOPS, Grad. Sch. Sci.,  
Univ. Tokyo, Tokyo 113-0033*

The JAXA's Hayabusa2 spacecraft explored C-type near-Earth asteroid (162173) Ryugu and successfully returned its reentry capsule on December 6, 2020. Particles exceeding ~5 grams in total were safely extracted from two sample chambers in the clean chamber system dedicated to Ryugu samples [1, 2]. After a six-month preliminary examination without exposure to the air by the JAXA Astromaterials Research Group (ASRG), a part of Ryugu samples have been studied by the initial analysis team led by the Hayabusa2 project [3]. Some samples have also been characterized by Phase-2 curation teams outside ASRG [4]. The rest of the samples are continued to be investigated in the clean chamber to be catalogued in a curatorial database system for Ryugu samples (Ryugu DBS), which will be archived to the community in early 2022 for the announcement of opportunity (AO). In this presentation, we report the aim and features of the Ryugu DBS.

The Ryugu DBS has been designed and built to provide the Ryugu sample catalog with the research community and to help the researchers make the sample request through the announcement of opportunity.

The concept design of the Ryugu DBS was made in mid 2019 based on lessons-learned from the operation of DBS for Itokawa samples (Itokawa DBS) [5]. A mockup was first made to check the web interface and the user-friendliness of the system in early 2020. The database system was then developed based on the feedback from the mockup review in Oct. 2020. The system has been used by limited members for further feedback, major updates were made, and a supplemental system such as a data input system was also developed. The Ryugu DBS is run using opensource technologies, such as PHP, PostgreSQL, and Apache, and data servers on Data ARchives and Transmission System (DARTS) at ISAS/JAXA.

The Ryugu DBS provides the information on each individual grain (typically larger than 1 mm along the longest dimension) and on aggregate samples. Because of the presence of large amount of fine particles (relative to Itokawa particles), fine grains are planned to be examined as an aggregate sample put in a single dish. The basic information listed in the DBS includes photomicrographs, weight, size, and spectroscopic data, all of which are obtained in the clean chamber system without exposure to the air. The spectroscopic data can be downloaded with the CSV format. Along with such basic information, the analysis history and data obtained in previous analysis can also be found for each sample. The data obtained by the project-led initial analysis and that from curation work outside JAXA will also be archived in the future.

The release of the Ryugu DBS to the community will be in early 2022.

## References

- [1] Tachibana S. et al. (2021) *LPS, XXXXXII*, Abstract #1289. [2] Yada T. et al. (2021) *LPS, XXXXXII*, Abstract #2008. [3] Tachibana S. et al. (2021) submitting for Hayabusa 2021 symposium. [4] Ito M. et al. (2021) submitting for Hayabusa 2021 symposium. [5] Uesugi M et al. (2016) *Journal of Space Science Informatics Japan: Vol 5, 59-70*.

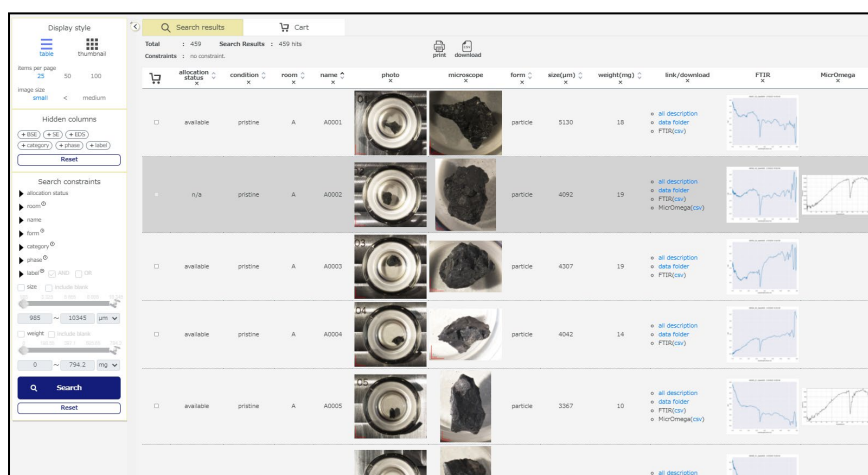


Fig. 1. The interface of the Ryugu DBS.

# Methodology of MicrOmega data acquisition/processing in initial description of Ryugu returned samples

Kasumi Yogata<sup>1</sup>, Tatsuaki Okada<sup>1,2</sup>, Kentaro Hatakeda<sup>1,3</sup>, Toru Yada<sup>1</sup>, Masahiro Nishimura<sup>1</sup>, Aiko Nakato<sup>1</sup>, Akiko Miyazaki<sup>1</sup>, Kazuya Kumagai<sup>1,3</sup>, Yuya Hitomi<sup>1,3</sup>, Hiromichi Soejima<sup>1,3</sup>, Kana Nagashima<sup>1</sup>, Ritsuko Sawada<sup>1,3</sup>, Shogo Tachibana<sup>1,2</sup>, Masanao Abe<sup>1,4</sup>, Tomohiro Usui<sup>1</sup>, Jean-Pierre Bibring<sup>5</sup>, Cedric Pilorget<sup>5</sup>, Vincent Hamm<sup>5</sup>, Rosario Brunetto<sup>5</sup>, Damien Loizeau<sup>5</sup>, Lucie Riu<sup>1,5</sup>, Lionel Lourit<sup>5</sup>, Guillaume Lequertier<sup>5</sup>, and Hayabusa2 MicrOmega-Curation team<sup>1,5</sup>

<sup>1</sup>Institute of Space and Astronautical Science, Japan Aerospace Exploration Agency, <sup>2</sup>University of Tokyo, <sup>3</sup>Marine Works Japan, Ltd., <sup>4</sup>The Graduate University for Advanced Studies (SOKENDAI), <sup>5</sup>Institut d'Astrophysique Spatiale, Université Paris-Saclay

The Hayabusa2 spacecraft successfully brought samples back to Earth in December 2020, collected at two different locations on the surface of the C-type asteroid Ryugu. The samples, weighing about 5.4 g, have been transported to the Extraterrestrial Samples Curation Center of JAXA and have been installed in vacuum chambers or pure nitrogen-purged chambers. JAXA curation is currently in the progress of producing catalog data to be included in the database, which is planned to be open in early 2022 towards sample allocation for Announcement of Opportunity [2]. Within this work, basic properties of return samples, for both the aggregate and individually picked-up grains, are acquired using microscopy, weighing, and visible/near-infrared spectroscopy and imaging analyzer. One of the methods is near-infrared hyperspectral microscopy by MicrOmega, developed at IAS (Orsay, France) [3].

MicrOmega is installed in a class 1000 clean room, in contact with a sapphire viewport window of a nitrogen-purged clean chamber. By distant monochromatic light illumination of MicrOmega, it enables non-destructive ultraclean analysis without exposure of the samples to the atmosphere and protecting them from contamination such as water and human-derived organics. MicrOmega has a 5x5 mm Field of View (FOV) and 250x256 pixels with a resolution of 22.5  $\mu\text{m}/\text{pixel}$ , and generates a hyperspectral  $(x, y, \lambda)$  cube within the 0.99 to 3.65  $\mu\text{m}$  wavelength range. The performance above can mark the presence of absorption bands suggestive of hydrous minerals at 1.4, 1.9, and 2.7-3.0  $\mu\text{m}$ , and of organics and carbonates at 3.4  $\mu\text{m}$ . Also, its FOV can cover the entire body of a single grain, most of which are about a few mm in size, and the image resolution allows to distinguish interstitial materials such as meteoritic inclusions more than 50-100  $\mu\text{m}$  in diameter.

In the production of data for the catalog, it is important to be careful about the shape-dependent signals of grains. The image often shows strong specular reflection and/or the shadow effect at a certain angle due to the instrument's light illumination incidence angle: 35 degrees. Therefore, for the catalog, two monochromatic images with different angles are generated for each single grain to show the effect of angular dependence. In addition, since the FOV usually includes signal from the sapphire sample dish where the grain sits, we extract the average spectra of the grain area only. Furthermore, if there are areas that show distinctive signatures different from most of the others, specific ROIs are also extracted. The database will contain images showing the ROIs and their spectral data, with comments on the inclusions and minerals they may imply.

In this presentation, we will introduce the MicrOmega data acquisition and data processing, including approaches in the presence of angle-dependent effects and sorting strategies for the curatorial initial description, and the characteristics of typical samples based on results obtained so far for each individual grain.

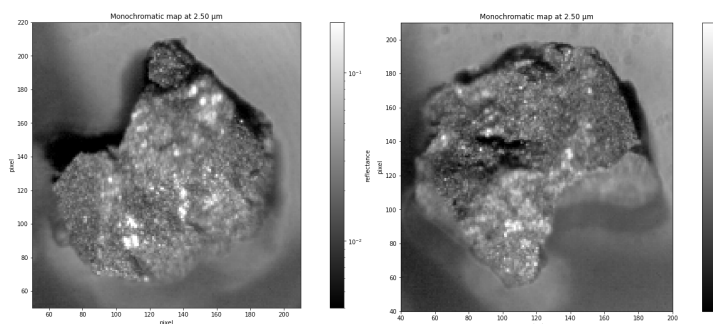


Figure 1. (a) Monochromatic image of A0015 grain at 2.50 $\mu\text{m}$  at 0 deg, and (b) at 180 deg, showing angular dependence on the reflectance.

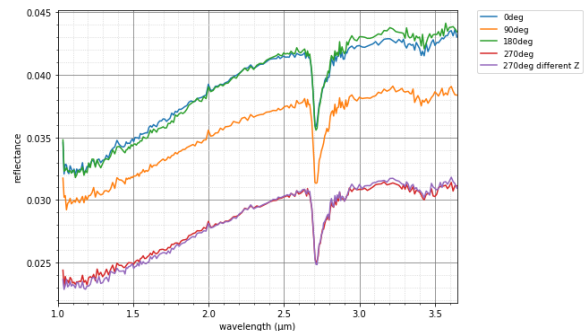


Figure 2. Average reflectance of A0015 at different angles and focal positions.

**References:** [1] Yada et al. submitted to Nature Astron., [2] Nishimura M. et al. (2021), Astromaterials Data Management in the Era of Sample-Return Missions Community Workshop, Abstract, [3] Pilorget et al. submitted to Nature Astron.

# Comparison of ion- and laser-weathered spectra of olivines and pyroxenes

K. Chrbolková<sup>1,2,3</sup>, R. Brunetto<sup>4</sup>, J. Ďurech<sup>2</sup>, T. Kohout<sup>1,3</sup>, K. Mizohata<sup>5</sup>, P. Malý<sup>6</sup>, V. Dědič<sup>7</sup>, C. Lantz<sup>4</sup>, A. Penttilä<sup>8</sup>, F. Trojánek<sup>6</sup>, and A. Maturilli<sup>9</sup>

<sup>1</sup>*Department of Geosciences and Geography, University of Helsinki, Gustaf Hällströmin katu 2, 00560 Helsinki, Finland*  
([katerina.chrbolkova@helsinki.fi](mailto:katerina.chrbolkova@helsinki.fi))

<sup>2</sup>*Astronomical Institute of Charles University, V Holešovičkách 2, 18000 Prague 8, Czech Republic*

<sup>3</sup>*Institute of Geology, The Czech Academy of Sciences, Rozvojová 269, 16500 Prague 6, Czech Republic*

<sup>4</sup>*Université Paris-Saclay, CNRS, Institut d'Astrophysique Spatiale, 91405 Orsay, France*

<sup>5</sup>*Department of Physics, Faculty of Science, University of Helsinki, Pietari Kalmin katu 2, 00560 Helsinki, Finland*

<sup>6</sup>*Department of Chemical Physics and Optics, Faculty of Mathematics and Physics, Charles University, Ke Karlovu 3, 12116 Prague, Czech Republic*

<sup>7</sup>*Institute of Physics, Faculty of Mathematics and Physics, Charles University, Ke Karlovu 5, 12116 Prague, Czech Republic*

<sup>8</sup>*Department of Physics, Faculty of Science, University of Helsinki, Gustaf Hällströmin katu 2, 00560 Helsinki, Finland*

<sup>9</sup>*Institute of Planetary Research, DLR German Aerospace Centre, Rutherfordstrasse 2, 12489 Berlin, Germany*

**Introduction:** Irradiation by solar wind ions and impacts of micrometeoroids are the leading processes that weather surfaces of airless planetary bodies in the solar system. As a result, key diagnostic features of their spectra get altered. The most prominent changes in the silicate-rich bodies in the visible (VIS) and near-infrared (NIR) wavelengths are increase in the spectral slope, reduction of the albedo, and flattening of the mineral absorption bands (see, for example, [1]).

Our laboratory experiments aimed at understanding what are the similarities and differences between the effect of the solar wind ions and micrometeoroid impacts on the final spectra of the silicate-rich bodies.

**Methods:** We have used two different terrestrial minerals, olivine and pyroxene, which we ground, dry-sieved, and pressed into pellets.

Hydrogen (H) irradiations proceeded at the Accelerator Laboratory of the University of Helsinki, using 5 keV ions with varying fluences from  $10^{14}$  to  $10^{18}$  ions/cm<sup>2</sup>. Helium and argon irradiations were done using the INGMAR set-up (IAS-CSNSM, Orsay) with 20 and 40 keV ions and with fluences from  $10^{15}$  to  $10^{17}$  ions/cm<sup>2</sup>.

Individual 100-fs laser pulses were shot into a square grid on the pellets' surface to simulate the micrometeoroid impacts (as in [2]) in the laboratories at Charles University. Various densities of the pulses per cm<sup>2</sup> simulated different weathering stages.

Subsequent spectral measurements covered wavelengths from 0.54 to 13  $\mu\text{m}$ , i.e. VIS to mid-infrared wavelengths. After the measurements, we evaluated the evolution of the spectral parameters estimated using the Modified Gaussian Model [3, 4].

**Results:** We found that the variation of the spectra in the VIS range was similar for H+- and laser-irradiated samples, but we have identified a difference in the NIR wavelength range. Laser irradiation caused greater changes in NIR than any of the ions we used, see Fig. 1. The reason for such difference in behaviour may be that the penetration depth of the laser pulses is much larger than in the case of the ions. The relative contribution of the irradiated material in the spectra is then smaller in the ion case than in the laser case.

Otherwise, we found that the original mineralogy of the surface is the leading factor influencing the evolution of the spectral parameters. While olivine and pyroxene showed albedo variations of a similar order, the evolution of pyroxene's spectral slope was negligible when compared to olivine. This has implications for olivine-pyroxene mixtures and their evolution. E.g. in the case of asteroid (433) Eros, the variation of the spectral slope is minor, but other spectral parameters show some variation. As the surface of Eros is old, we hypothesise that spectral slope changes induced by olivine alteration already saturated and the leading source of the spectral variation is pyroxene, which does not show large variations in the slope. In contrast asteroid (25143) Itokawa is younger and thus still shows variations in the spectral slope as it has not saturated yet.

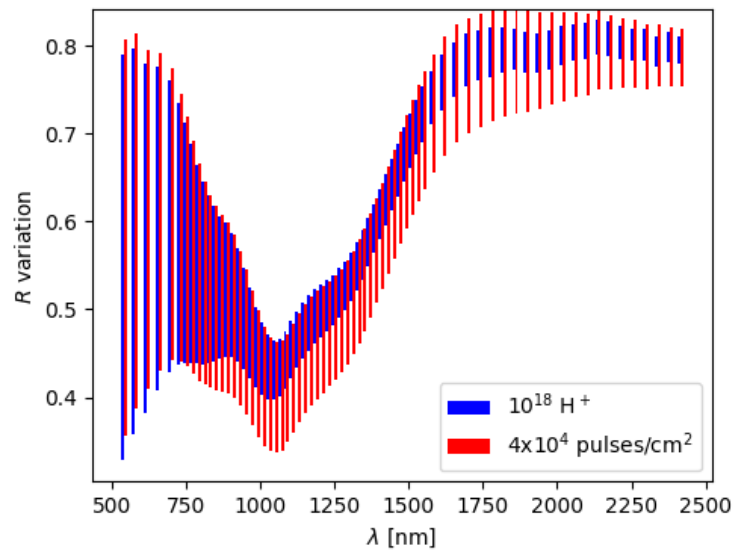


Figure 1. Spectral differences caused by laser and hydrogen ion (H<sup>+</sup>) irradiation. Each bar connects at the upper end the reflectance, *R*, of the fresh material and at the lower end *R* of the material weathered to the level marked in the legend.

### References

- [1] Hapke, B. 2001, *J. Geophys. Res.*, 106, 10039
- [2] Fazio, A., Harries, D., Matthäus, G., et al. 2018, *Icarus*, 299, 240
- [3] Sunshine, J. M., Pieters, C. M., & Pratt, S. F. 1990, *J. Geophys. Res.*, 95, 6955
- [4] Sunshine, J. M., Pieters, C. M., Pratt, S. F., & McNaron-Brown, K. S. 1999, in *Lunar and Planetary Inst. Technical Report*, Vol. 30, Lunar and Planetary Science Conference, 1306

# Solid Materials of Mineral and Rock on the Solar System: X-ray Unit and Mixed Status

Yasunori Miura<sup>1</sup> and Toshio Kato<sup>2</sup>

<sup>1</sup>*Faculty of Science, Yamaguchi University, Yoshida, Yamaguchi, Yamaguchi, JAPAN*

<sup>2</sup>*Department of Earth System Sciences, Faculty of Science, Yamaguchi University, Yoshida, Yamaguchi, Yamaguchi, JAPAN*

**Introduction:** Solid materials of all celestial bodies on the Solar System (with technical limits of whole observation and collection by man-made satellites) should be *defined clearly* as main purpose of this paper based on academic data of those solids from the Earth's definition relatively.

**Academic definition:** All *mineral crystals* on Earth are defined with *X-ray determination* (as arrangement of 0.1nm unit) and *chemical composition* (as stoichiometric compound) with its occurrence on the academic material database (as *Earth's mineral*), where *the rock* is composed on many mineral crystals or mineral with mixed irregular solids (with light or heavy elements) usually. This *Earth's definition* is easily applied to investigate and determination to unknown samples including extraterrestrial samples on Earth and visiting collections on the Moon (and Mars and Asteroids *etc.*). However, basic definition of *solid samples on extraterrestrial sources* is not enough to be defined (especially on its developed status as the Celestial bodies) as shown in Table 1.

**New concept of the Solar System's material:** Solid bodies of the Solar System have been accepted mainly from their movements from *the geo-centered theory* to the *Helio-centered theory* through many astrophysical investigators based on the Moon and nearest planetary *tracking data*. Therefore, we should investigate by solid *material database* (rock and/or mineral crystal) of *each Celestial body*. This is main reason why a) mineral spices are completely different with the water-planet Earth (three systems of rock, ocean water and atmosphere as the mineral differentiation) and other Celestial bodies (mainly rock and/or atmosphere systems as different generation of mineral and rock compared with the planet Earth), b) previous collected extraterrestrial rocks (without chondrules or not) shows different evolution of glass and mineral, c) final mineral grains (soils, carbonates and silica) of the Earth's sedimentary process cannot be obtained clearly on extraterrestrial samples so far, and d) various mineral deposits of light element of carbon (from extreme to lower conditions) are obtained from macroscopic to microscopically as shown in Table 1.

Table 1. Different concepts of the Solar System's materials discussed in this study.

Celestial body	Mineral crystal	Rock
1) Earth (water-planet)	X-ray atomic structure & stoichiometric chemistry	Its mixed texture (with glass etc.)
2) The Moon	Shocked reformed minerals	Amorphous or mixed minerals
3) Mars	Mainly shocked minerals (with fluid products)	Basaltic evolved rocks (with glasses)
4) Asteroids	Mainly shocked minerals (with reacted vapors)	Shocked chondritic/growth grains

**Existence of fluid-related grains:** Carbon-bearing grains show only *light element* to exist all phase states from solid to liquid to vapor condition with various compositions, texture and atomic structure. Therefore, it is *significant indicator* to detect its formed process with or without fluid on *water-planet Earth* (to form final *global carbonate minerals* and its rocks), the Moon (to form *global carbon distribution* rich in fine regolith soils on surface), Mars (to form *global carbon-rich grains* and deposits) and Asteroids (*carbon-rich in fine regolith* grains and/or *carbon-bearing grains* and rocks) as shown in Table 2.

**Discussion:** Earth's minerals formed as large mineral crystals are defined by atomic structure and chemistry based on X-ray analysis and EPMA-A TEM/SEM microanalyses in laboratory on Earth. On the other hand, extraterrestrial samples of the Moon, Mars and Asteroids have no large crystal of mineral grains (due to no global water system on these bodies). Therefore, Earth's mineral crystal cannot be obtained at any other planets and Asteroids without the global water system. Remote-sensing detectors by the IR and Visible wavelengths are mainly instant data obtained from mainly molecular data (atom-atom distances) which are different with Earth's mineral definition. This suggests that extraterrestrial mineral rocks (or rocky minerals) are considered to be *imperfect solids* compared with Earth-type mineral crystal, which means that *main X-ray peaks* of crystal planes (hkl) are mainly formed during the developed processes with short extreme condition of simple or multiple impact heating and cooling processes on the extraterrestrial bodies. In short, all celestial bodies at the Solar System are

completely different on its process and fluid contribution for rocky mineral or mineral rock formation (including the Hayabusa samples), which means that solid bodies of the Solar System might be the *Helio-centered theory-type* material rocks which are not used by the Earth-type mineral rocks to all other extraterrestrial bodies (not as the Earth (geo)-centered materials as used in the astronomical scale previously).

Table 2. Carbon-bearing and/or -rich grains and/or rocks of the Solar System's materials discussed in this study.

Celestial body	Carbon-bearing and/or -rich grains and/or rocks
1) Earth (water-planet)	Final global carbonate minerals and rocks and life/plant solidified rocks (shungite <i>etc.</i> )
2) The Moon	Global carbon distribution rich in fine regolith soils on surface (with shocked grains)
3) Mars	Global carbon-rich grains and deposits (with shocked grains)
4) Asteroids	Fine carbon-rich regolith grains and/or carbon-bearing grains and its rocks

**Summary:** The following data are summarized in this study. 1) Solid materials of all Celestial bodies on the Solar System are discussed on the solid data from the *Earth's definition* relatively to the extraterrestrial Celestial bodies. 2) All mineral crystals on Earth are defined with X-ray determination and chemical composition with its occurrence on the material database, though basic definition of extraterrestrial sample is not enough to be defined from *less crystalline* rocks. 3) The Earth's minerals show absolutely *huge numbers* of mineral species, *well differentiated* minerals, *various Earth's sedimentary* process, and *various mineral* deposits of *carbon-bearing* grains. 4) Carbon-bearing grains show various grains, texture and compounds which are indicators of the detailed *formation process* on each Celestial body including the Hayabusa samples. 5) The material data of the samples might indicate that all material data of mineral and rock are different from the Celestial bodies of the Solar System.

#### References:

- Cresswell R., Beukens R., Rucklidge J. and Miura Y., Distinguishing spallogenic from non-spallogenic carbon in chondrites using gas and temperature separations. Nuclear Instruments and Methods in Physics Research Section B (NIM-B) (Elsevier Science, North-Holland), 92, 505-509, 1994.
- Kato T. and Miura Y., The crystal structures of Jarosite and svanbergite. Mineralogical Journal, 8, 419-430, 1977.
- Miura Y., Comparative consideration of Earth's mineral from three major events: Solid formation of other Celestial bodies, JAMS-2021 (Hiroshima Univ.), R5-01, 2021.
- Miura Y., Carbon and carbon dioxides gas fixing by dynamic processes, Publication of JP5958889B2 (Active to 2028), 2016.
- Miura Y., Complex texture and structure of shocked quartz mineral with graphite grain., Acta Cryst., 64, 55, 2008.
- Miura Y., Material evidence for compositional change of dusts by collision applied to the Solar System's formation and the Asteroid belt. The ASP Conf. Series, 63, 286-288, 1994.
- Miura Y. and Kato T., Shock waves in cosmic space and planetary materials. American Institute of Physics (AIP) Conf. Proc., 283 (Earth and Space Science Information Systems), 488-492, 1993.
- Miura Y., Accelerator mass spectrometry facilities in Japan. The Future of AMS Requirements in Canada (NSERC), 1, 45, 1991.
- Miura Y. and Tomisaka T., Composition and structural substitution of meteoritic plagioclases. Mem. Natl Inst. Polar Res., Spec. Issue (NIPR, Tokyo), 35, 210-225, 1984.
- Miura Y., Computer simulation of anomalous composition of Mg-Fe plagioclase in meteorite. Mem. Natl Inst. Polar Res., Spec. Issue (NIPR, Tokyo), 35, 226-242, 1984.
- Smith D.G.W., Miura Y. and Launspach S., Fe, Ni and Co variations in the metals of some Antarctic chondrites. Earth and Planetary Science Letters, 120, 487-498, 1993.

# Model of Material Characteristics of Carbonaceous Meteorites from Texture of Carbon-Bearing Grains

Yasunori Miura

*Faculty of Science, Yamaguchi University, Yoshida, Yamaguchi, Yamaguchi, JAPAN*

**Introduction:** Carbonaceous meteorites are unique meteorites in the extraterrestrial rocks. In this study author reports proposed model of previous unknown characteristics of *hard samples with voids, carbon-bearing texture, Ca-Al-rich grains* (with H, C, S) and detailed model of *carbon-bearing grains* in the carbonaceous meteorite which are applied to the Hayabusa samples as the present purpose here.

**Characteristics of Carbonaceous chondrite:** Carbonaceous chondrites contain usually Ca and C elements (with Mg, Na ions and H<sub>2</sub>O molecules), where these ions can form molecular *gel (polymer)* and *amorphous* (poorly crystallized Embryo-type of *carbonates* (calcite and aragonite in mineral crystal). This suggests that extraterrestrial Celestial body is started as 1) *Ordinary chondrite-type micrograins* and *intercluster pores* (as less 2nm) followed *gel pores* (2 to 20nm in size) without carbonated calcium silicate matrixes, and 2) *Carbonaceous chondrite-type micrograins* show Ca-modified silica *gel clusters* mixed with *amorphous calcium carbonates (ACC)* with pores (4 to 10nm) as shown in Table 1. This model can be explain why the meteorite shows *porous rocks* and *harder rock* (than normal porous crystalline rocks with light weight). These gel to amorphous grain can be formed in present laboratory and industrial application as *Ca-Al-rich grains* (with H, C, S) as low *carbon binders*. This is just by accident in natural meteorite field academically because author has been investigated carbon origin and its application in science filed (including the AMS carbon dating projects) used in terrestrial age of the Antarctic meteorites (also in the Apollo samples as its carbon origins), and recent project of carbon and *carbon dioxides gas fixing* by dynamic processes (as the public University project). If it can be confirmed in science filed, then we can apply that *carbonaceous meteorites* (and Moon rocks) has similar texture to fix carbon (or carbon dioxides) by its sources and development of its *extraterrestrial rocks* (model of grains of ions-gel polymer-amorphouse calcium carbonates as shown in Table 1, followed clear calcite crystal as in water planet Earth finally). This can be applied it also to decrease the *climate warning* scientifically and inductrially (as well-known Japanese scientist indicated by calculated estimates from global environmental data). The paper is dicussed it as material data with proposed model in the Hayabusa Symposium in Tokyo.

Table 1. Proposed model of micro-grains with pores from of the Solar System.

Meteorite variety	Micro-structure
1) Ordinary chondrite	Micro-grains and inter-cluster pores (as less 2nm), gel pores (2 ~ 20nm in size) (less carbonated calcium silicate matrixes)
2) Carbonaceous chondrite	Micro-grains with Ca-modified silica gel clusters mixed with amorphous calcium carbonates (ACC) with pores (4 to 10nm)

**Summary:** Author proposes model of hard samples with voids, carbon-bearing texture, Ca-Al-rich grains (with H, C, S) and carbon-bearing grains in the carbonaceous meteorite (also including the Hayabusa samples).

**References:**

Miura Y., Comparative consideration of Earth's mineral from three major events: Solid formation of other Celestial bodies, JAMS-2021 (Hiroshima Univ.), R5-01, 2021.

Miura Y., Carbon and carbon dioxides gas fixing by dynamic processes, Publication of JP5958889B2 (Active to 2028), 2016.

Miura Y. and Tanosaki T., Characterization of products from the nuclear and fire-electric facilities (in Japanese), University Report (Yamaguchi, Japan), 1-64, 2009.

Miura Y., Material evidence for compositional change of dusts by collision applied to the Solar System's formation and the Asteroid belt. The ASP Conf. Series, 63, 286-288, 1994.

Miura Y. and Kato T., Shock waves in cosmic space and planetary materials. American Institute of Physics (AIP) Conf. Proc., 283 (Earth and Space Science Information Systems), 488-492, 1993.

Smith D.G.W., Miura Y. and Launspach S., Fe, Ni and Co variations in the metals of some Antarctic chondrites. Earth and Planetary Science Letters, 120, 487-498, 1993.

Miura Y., Computer simulation of anomalous composition of Mg-Fe plagioclase in meteorite. Mem. Natl Inst. Polar Res., Spec. Issue (NIPR, Tokyo), 35, 210-242, 1984.

# Neural network for classification of asteroid spectra

David Korda<sup>1</sup>, Antti Penttilä<sup>2</sup>, Arto Klami<sup>3</sup>, and Tomáš Kohout<sup>1,4</sup>

<sup>1</sup>Department of Geosciences and Geography, University of Helsinki, Finland

<sup>2</sup>Department of Physics, University of Helsinki, Finland

<sup>3</sup>Department of Computer Science, University of Helsinki, Finland

<sup>4</sup>Institute of Geology, Czech Academy of Sciences, Czech Republic

## Introduction

Asteroid mineral composition is important parameter in planetary science, planetary defence, and in-space resource utilisation. Currently-used methods provide us mainly quantitative information about the asteroid composition. The methods are based on empirical relations between spectral parameters (band areas, positions, depths), or on spectral unmixing, and are highly sensitive to quality and consistency of input reflectance spectra. We test artificial neural networks as a tool which can infer mineral composition directly from the reflectance values.

## Methods

Artificial neural networks are used in tasks which are very difficult to define with exact mathematics. A sensitivity of the networks to quality of input data (e.g., absolute reflectance values or variations in spectral slope) can be partially suppressed. The networks are made of layers of neurons. Each neuron in a layer is non-linearly connected with neurons in the previous and following layers. The non-linearity and complexity of neural network enable them to solve various tasks.

We use neural network for computing of mineral composition of the most common silicates presented in meteorites (olivine, orthopyroxene, clinopyroxene, and plagioclase). Our neural network composed of the input layer with reflectance values, one ‘intermediate’ layer (hidden layer), and the output layer. The outputs are modal composition of the minerals and their chemical composition represented with end-members.

## Data

We utilised measured reflectance spectra from the Relab database<sup>[1]</sup>. We are motivated by the ASPECT instrument (part of Hera/Milany CubSat) which will carry-out observations in visible and near-infrared part of spectra. For this reason, we chose spectra which cover interval between 350 nm and 2550 nm with the resolution 15 nm or better.

## Results

Olivine and orthopyroxene are the most common minerals in ordinary chondrites. Therefore, we firstly applied the neural network on a set of olivine and pyroxene spectra.

---

<sup>1</sup><http://www.planetary.brown.edu/relabdata/>

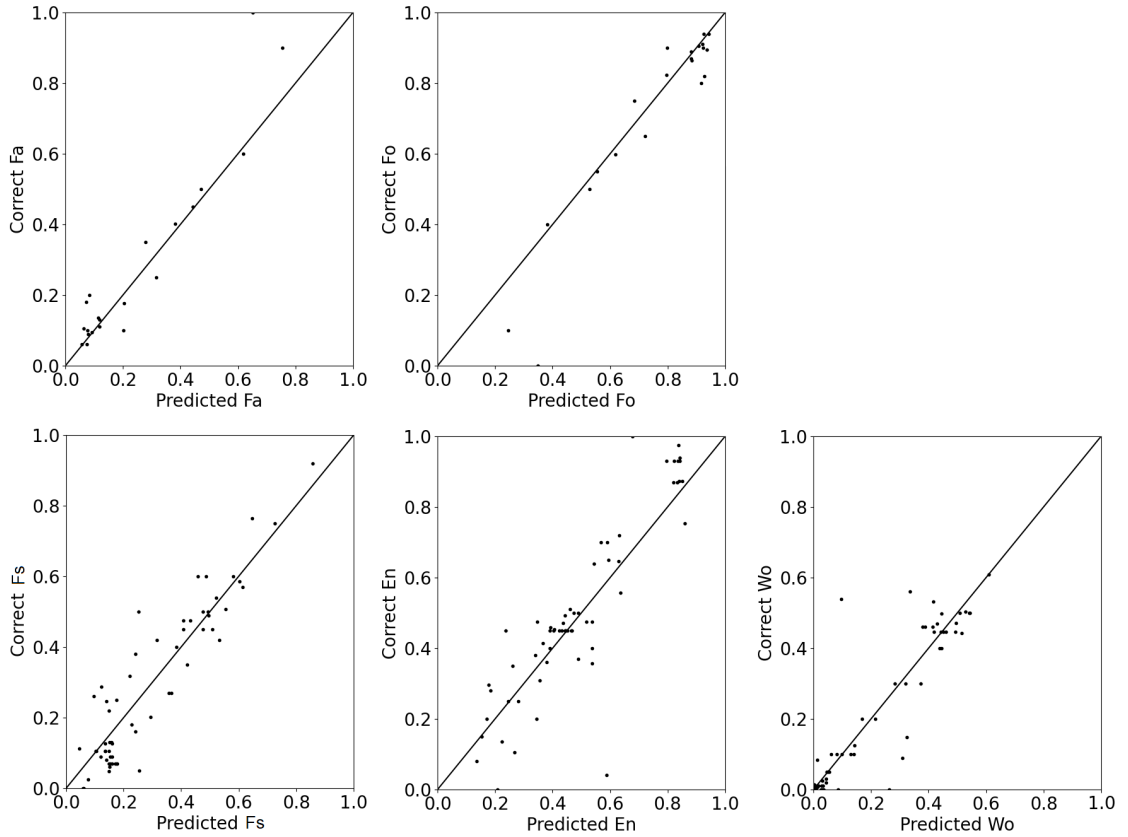


Figure 1: Results of chemical composition. Top row: olivine. Bottom row: pyroxene.

The neural network contained only one hidden layer with 30 neurons. The outputs were volume fractions of the minerals and their chemical composition. We trained the network on about 80% of the whole dataset and used the remaining 20% to test the accuracy of the predictions. The results obtained from the 20% are shown in Fig. 1. The vertical axes show the correct (previously published) values while the horizontal axes the values predicted by the neural network. In the top row, there are iron and magnesium composition in olivine. In the bottom row, there are iron, magnesium, and calcium composition in pyroxene.

## Discussion

Except a few outlier, the predicted composition is usually within about 10% from the actual composition. The outliers might be a consequence of a limited training dataset or ambiguously determined actual composition. In the near future, the predictive capability of the network will be improved via optimisation of its architecture and due to increase number of training samples. In the next step, we will train the network on synthetic spectra of olivine, orthopyroxene, and plagioclase and evaluate the network on real ordinary chondrites.

## Assessment of organic, inorganic and microbial contamination in the facilities of the Extraterrestrial Sample Curation Center of JAXA

\*Yuya Hitomi<sup>1</sup>, Toru Yada<sup>2</sup>, Aiko Nakato<sup>2</sup>, Miwa Yoshitake<sup>1,3</sup>, Kana Nagashima<sup>2</sup>, Haruna Sugahara<sup>2</sup>, Shino Suzuki<sup>2</sup>, Masahiro Nishimura<sup>2</sup>, Kazuya Kumagai<sup>1</sup>, Masanao Abe<sup>2</sup>, Tatsuaki Okada<sup>2</sup>, Shogo Tachibana<sup>2,4</sup>, and Tomohiro Usui<sup>2</sup>

<sup>1</sup>Marine Works Japan Ltd., Yokosuka, Kanagawa 237-0063, Japan, <sup>2</sup>Institute of Space and Astronautical Science (ISAS), Japan Aerospace Exploration Agency, Sagami-hara, Kanagawa 252-5210 Japan, <sup>3</sup>Japan Patent Office, Chiyoda-ku, Tokyo 100-8915, Japan, <sup>4</sup>UTOPS, Grad. Sch. Sci., Univ. Tokyo, Tokyo 113-0033, Japan.

The Extraterrestrial Sample Curation Center of JAXA (ESCuC) have received samples from S-type near-Earth asteroid 25143 Itokawa returned by Hayabusa and C-type near-Earth asteroid 162173 Ryugu by Hayabusa2 [1, 2]. The samples have been taken out from sample containers, investigated in a non-destructive way, and stored in high vacuum and purified nitrogen circulating clean chambers installed in ISO Class 6 clean rooms in the ESCuC. A series of cleaning procedures for tools, jigs, and sample storage/transport containers has been established for the usage in the clean chambers to avoid potential contamination of samples [3].

Along with the contamination control, it is also important to keep monitoring the cleanliness of clean rooms and clean chambers. For instance, several biotic amino acids were once detected from contamination coupons set inside the clean chamber for Itokawa grains [4], of which contamination level was similar to that reported at the curation facility at NASA Johnson Space Center [5, 6]. In recent years, contamination of organics has been assessed regularly through exposure of wafers for 15-20 hours in the clean rooms and clean chambers. The regular assessment has found that the clean rooms is kept at the ISO-SCC Class -8 level and the clean chambers at the ISO-SCC Class -9 for organics. Regular contamination assessment of metallic elements has shown that both clean rooms and clean chambers maintain the level of ISO-SCC Class -10 or higher for all measured elements although elements contained in equipments and tools, such as Fe, Cu, Ni, Cr, Al, Zn, Mn, and Co, were often detected at a higher level in the clean chambers than in the cleanrooms. The contamination levels of Na and K, both of which are good indicators of contamination from human beings, are low enough to be at the ISO-SCC class -11 level for both clean chambers and cleanrooms. In addition to organic and inorganic monitoring, assessment of microbial contamination level is scheduled for the cleanrooms and clean chambers in this fiscal year.

### References

[1] Yada T. et al. (2014) *Meteoritics Planet. Sci.* 49, 135-153. [2] Yada, T. et al. (2021) LPSC 52, #2008. [3] Yoshitake M. et al. (2021) JAXA-RR-20-004E, 1-30. [4] Sugahara H. et al. (2018) *Earth Planets Space* 70, 194. [5] Dworkin et al. (2018) OSIRIS-REx contamination control strategy and implementation. *Space Sci Rev* 214:9. [6] McLain et al. (2015) Contamination Knowledge Report JSC Curation Cabinets, personal communication.